

Iodosylbenzene Oxidation of Alkanes, Alkenes, and Sulfides Catalyzed by Binuclear Non-heme Iron Systems: Comparison of Non-heme Iron Versus Heme Iron Oxidation Pathways

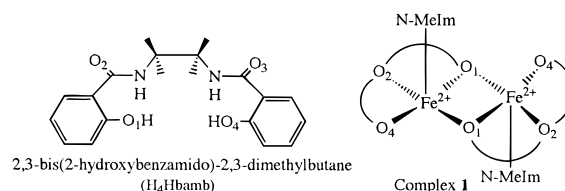
Subhasish Mukerjee, Adonis Stassinopoulos, and John P. Caradonna*

Department of Chemistry, Kline Laboratory
Yale University, P.O. Box 208107
New Haven, Connecticut 06520-8107

Received March 25, 1997

Understanding the mechanisms by which binuclear non-heme iron centers such as those found in the active site of methane monooxygenase (MMO) can act as oxygen atom transfer catalysts remains a serious and complex challenge.^{1,2} Despite recent major advances in our understanding of the structural,³ spectroscopic,^{4,5} and mechanistic aspects of enzymatic alkane oxidation,^{4,5} attempts to model biological hydrocarbon oxidation are less well developed.^{1,2} While synthetic non-heme diferric systems are reported to oxygenate substrates in the presence of either dioxygen⁶ or alkyl peroxides,^{1,2,4,5,7–13} the peroxide chemistry is now thought to be dominated by oxygen-based free radical pathways.^{14–17} In our continuing efforts to develop catalytically competent binuclear non-heme Fe complexes that can perform biologically relevant oxo-atom transfer chemistry,^{18,19} we report herein the remarkable reactivity properties of $[\text{Fe}_2^{2+}(\text{H}_2\text{Hbamb})_2(\text{N-MeIm})_2]$ (**1**, Scheme 1),^{20a} as well as those of its mixed-valence $[\text{Fe}^{2+}, \text{Fe}^{3+}]$ (**2**) and diferric $[\text{Fe}^{3+}, \text{Fe}^{3+}]$ (**3**) states. We find that both **1** and **2** are uniquely capable of catalyzing the oxidation of alkanes, alkenes, and sulfides by the known oxygen atom donor, OIPh. The catalytic chemistry of non-heme **1** and **2** parallel that reported for cytochrome P-450, a system believed to involve a porphyrin cation radical $[\text{Fe}^{4+}=\text{O}]$ reactive intermediate.^{21–23}

Scheme 1



The reaction of equimolar quantities of *trans*- $\text{Fe}^{2+}(\text{N-MeIm})_2(\text{Cl})_2(\text{MeOH})_2$ ^{18,19} and the dilithium salt of 2,3-bis(2-hydroxybenzamido)-2,3-dimethylbutane, H_4Hbamb (Scheme 1),²⁴ in anhydrous 1% methanol–acetonitrile under anaerobic conditions afforded $[\text{Fe}_2^{2+}(\text{H}_2\text{Hbamb})_2(\text{N-MeIm})_2]$ (**1**)^{25a} (60% yield). Isothermal distillation techniques¹⁸ indicate that **1** has a molecular weight of ≈ 1100 , consistent with its dimeric formulation. EPR spectra of **1** show a $g_{\text{eff}} \approx 16$ signal, suggesting a ferromagnetically coupled $S = 4$ core as previously reported for an analogously binuclear system.¹⁹ Cyclic voltammetry experiments show two coupled $1e^-$ oxidation/reduction processes; a scan-rate-dependent quasi-reversible process at -310 mV (NHE) and an electrochemically reversible couple at -690 mV (NHE), giving $K_{\text{com}} = 2.7 \times 10^6$. Repetitive scans showed no significant decrease in either cathodic or anodic current; ligand centered redox behavior was observed outside this region of interest. The scan-rate dependence of ΔE_p , attributed to kinetic effects, allowed the measurement of an intrinsic rate constant, $k = 2 \times 10^{-5}$, assuming pseudo-first-order kinetics. This rate constant, thought to reflect a structural change, is independent of **1** over a 3-fold range. A similar process was demonstrated in the redox transformation (-10 and -260 mV) of $[\text{Fe}_2^{2+}(\text{H}_2\text{Hbab})_2(\text{N-MeIm})_2]$.¹⁹ The stoichiometric I_2 titration of **1**, as monitored by UV/vis spectroscopy, shows the clean formation of $[\text{Fe}^{2+}, \text{Fe}^{3+}]$ (**2**) (isosbestic point at 325 nm); the titration of one additional oxidizing equivalent readily converts **2** to $[\text{Fe}^{3+}, \text{Fe}^{3+}]$ (**3**) (isosbestic points at 457 and 335 nm). Solution molecular weight characterizations of **2** and **3** are consistent

* Corresponding author. E-mail: john.caradonna@yale.edu.

(1) Caradonna, J. P.; Stassinopoulos, A. *Adv. Inorg. Biochem.* **1994**, *9*, 245–315.

(2) Stassinopoulos, A.; Mukerjee, S.; Caradonna, J. P. *Reactivity Models for Dinuclear Iron Metalloenzymes: Oxygen Atom Transfer Catalysis and Dioxygen Activation*; Stassinopoulos, A., Mukerjee, S., Caradonna, J. P., Eds.; American Chemical Society: Washington D.C., 1994; Vol. 246, pp 83–120.

(3) Rosenzweig, A. C.; Frederick, C. A.; Lippard, S. J.; Nordlund, P. *Nature* **1993**, *366*, 537–43.

(4) Feig, A. L.; Lippard, S. J. *Chem. Rev.* **1994**, *94*, 759–805.

(5) Waller, B. J.; Lipscomb, J. D. *Chem. Rev.* **1996**, *96*, 2625–2658.

(6) Rosenzweig, A. C.; Feng, X.; Lippard, S. J. *Applications of Enzyme Biotechnology*; Kelly, J. W., Baldwin, T. O., Eds.; Plenum Press: New York, 1991; pp 69–85.

(7) Barton, D. H. R.; Beck, A. H.; Taylor, D. K. *Tetrahedron* **1995**, *51*, 5245–5254.

(8) Vincent, J. M.; Menage, S.; Lambeaux, C.; Fontecave, M. *Tetrahedron Lett.* **1994**, *35*, 6287–6290.

(9) Kim, J.; Harrison, R. G.; Kim, C.; Que, L. J. *J. Am. Chem. Soc.* **1996**, *118*, 4373–4379.

(10) Perkins, M. J. *Chem. Soc. Rev.* **1996**, *25*, 229–236.

(11) Minisci, F.; Fontana, F.; Araneo, S.; Recupero, F.; Zhao, L. *SynLett* **1996**, 119–125.

(12) Arends, I. W. C. E.; Ingold, K. U.; Wayner, D. D. M. *J. Am. Chem. Soc.* **1995**, *117*, 4710–4711.

(13) Stassinopoulos, A.; Caradonna, J. P. *J. Am. Chem. Soc.* **1990**, *112*, 7071–7073.

(14) Stassinopoulos, A.; Schulte, G.; Papaefthymiou, G. C.; Caradonna, J. P. *J. Am. Chem. Soc.* **1991**, *113*, 8686–8697.

(15) Abbreviations: H_4Hbamb , 2,3-bis(2-hydroxybenzamido)-2,3-dimethylbutane; *N-MeIm*, *N*-methylimidazole; H_4Hbab , 1,2-bis(2-hydroxybenzamido)benzene; PPA, phenylperacetic acid; TPP, tetraphenylporphyrin.

(16) McMurry, T. J.; Groves, J. T. *Cyt P450 model systems*; McMurry, T. J., Groves, J. T., Eds.; Plenum Press: New York, 1986; pp 1–28.

(17) Sono, M.; Poach, M. P.; Coulter, E. D.; Dawson, J. H. *Heme-Containing Oxidases*; Sono, M., Poach, M. P., Coulter, E. D., Dawson, J. H., Eds.; American Chemical Society: Washington, D.C., 1996; Vol. 96, pp 2841–2888.

(18) Anson, F. C.; Christie, J. A.; Collins, T. J.; Coots, R. J.; Furutani, T. T.; Gipson, S. L.; Keech, J. T.; Kraft, T. E.; Santasiero, B. D.; Spies, G. H. *J. Am. Chem. Soc.* **1984**, *106*, 4460–4472.

(19) (a) $[\text{Fe}_2^{2+}(\text{H}_2\text{Hbamb})_2(\text{N-MeIm})_2]$ solvated (**1**): Anal. Calcd for $\text{C}_{55}\text{H}_{72}\text{N}_9\text{O}_{13}\text{Fe}_2$: C, 55.90; H, 6.10; N, 10.68; Fe, 9.49. Found: C, 55.69; H, 5.70; N, 10.86; Fe, 9.43. UV/vis (DMF): λ_{max} (ϵ_M) 314 nm (20 000). IR: ν_{amideNH} = 3430 cm^{-1} , ν_{amideCO} = 1611 cm^{-1} . Electrochemistry (NHE): quasi reversible redox process, -690 mV, $\Delta E = 220$ – 470 mV with scan rate 25–125 mV s^{-1} ; reversible process, -310 mV, $\Delta E = 70$ mV. (b) $[\text{Fe}^{2+}, \text{Fe}^{3+}(\text{H}_2\text{Hbamb})_2(\text{N-MeIm})_2](\text{I}^-)$ solvated (**2**): Anal. Calcd. for $\text{C}_{55}\text{H}_{72}\text{N}_9\text{O}_{15}\text{Cl}_2\text{Fe}_2$: C, 49.18; H, 5.36; N, 10.43; Fe, 8.31. Found: C, 48.67, H, 5.27; N, 10.37; Fe, 8.10. UV/vis (DMF): λ_{max} (ϵ_M) 301 nm (25 000), 436 nm (7000). IR: ν_{amideNH} = 3430 cm^{-1} ; ν_{amideCO} = 1654 cm^{-1} . EPR: $g_{\text{eff}} = 4.3$. (c) $[\text{Fe}_2^{3+}(\text{H}_2\text{Hbamb})_2(\text{N-MeIm})_2](\text{I}^-)_2$ solvated (**3**): Anal. Calcd. for $\text{C}_{55}\text{H}_{72}\text{N}_{10}\text{O}_{15}\text{I}_2\text{Cl}_2\text{Fe}_2$: C, 44.90, H, 4.90, N, 9.53, Fe, 7.60. Found: C, 44.22, H, 5.20, N, 9.71; Fe, 7.46. UV/vis (DMF): λ_{max} (ϵ_M) = 301 nm (25 000), 470 nm (7000). IR: ν_{amideNH} = 3430 cm^{-1} , ν_{amideCO} = 1654 cm^{-1} . Forms adduct with catechol DMF (λ_{max} = 560 nm).

(20) All gas chromatographic analysis were performed on a Hewlett-Packard Series 2 GC equipped with a methylsilicon capillary column and interfaced to a HP3396 series II integrator. Mass spectral analyses were performed on a HP 5971 mass-selective detector attached to a HP5890 Series 2 GC. Authentic samples were used to verify all retention times. Expected reaction products were stable to GC conditions.

(21) Studies using FeCl_2 and FeCl_3 were performed and analyzed by GC and GC/MS techniques using identical conditions as reported for **1–3** (Table 1) with catalyst:OIPh:substrate = 1:500:2500 ([catalyst] = 1 mM). All reactions were performed in 10% DMF/ CH_2Cl_2 under an inert (N_2) atmosphere and followed for 12 h.

(22) Cyclohexane and cyclohexane- d_{12} studies were performed in two separate reactions with OIPh and **1**; cyclooctane was used as an internal standard (1:OIPh:substrate = 1:500:2500, [1] = 1mM). The ratio of the product distribution of cyclohexanol:cyclooctanol and deuterated cyclohexanol:cyclooctanol yields the desired $k_{\text{H}}/k_{\text{D}}$.

(23) Liu, K.; Johnson, C. C.; Newcomb, M.; Lippard, S. J. *J. Am. Chem. Soc.* **1993**, *115*, 939–947.

(24) Rataj, M. J.; Kauth, J. E.; Donnelly, M. I. *J. Biol. Chem.* **1991**, *266*, 18684–18690.

(25) Green, J.; Dalton, H. *Biochem. J.* **1989**, *259*, 167–172.

(26) Groves, J. T.; Nemo, T. E. *J. Am. Chem. Soc.* **1983**, *105*, 6243–6248.

(27) Linsey Smith, J. R.; Mortimer, D. N. *J. Chem. Soc., Chem. Commun.* **1985**, 410–411.

Table 1. Catalytic Properties^a of [Fe²⁺,Fe^{m+}] Core Oxidation States Versus Iron Porphyrin Systems

substrate	products	[Fe ²⁺ ,Fe ²⁺] ^b T.O. ^f (eff %) ^g	[Fe ²⁺ ,Fe ³⁺] ^c T.O. ^f (eff %) ^g	[Fe ³⁺ ,Fe ³⁺] ^d T.O. ^f (eff %) ^g	Fe ³⁺ porphyrins ^e T.O. (yield %) ^h
cyclohexane	cyclohexanol	57 (44) ⁱ	1 (10)	— (3)	4 (31) ^j
	cyclohexanone	1	1	—	(6)
	chlorocyclohexane	49	38	13	
cyclohexene	cyclohexene oxide	83 (58) ^j	78 (64)	— (10)	5 (55) ^j
	cyclohexenol	100	127	5	(15)
	cyclohexenone	100	151	—	(1)
PhSMe	PhS(O)Me	3500 (93) ^k	600 (45)	—	84 (75) ^l
	PhS(O) ₂ Me	1000	2	—	(9)
toluene	benzyl alcohol	23 (35) ^j	1 (10)	1 (3)	1.2 (11) ^m
	benzaldehyde	5	—	1	1
	<i>o</i> -cresol	1	1	—	—
	<i>m</i> -cresol	1	19	—	—
	<i>p</i> -cresol	1	1	—	—

^a All reactions use OIPh as oxygen atom donor molecule. ^b Fe₂²⁺(H₂Hbamb)₂(*N*-MeIm)₂. ^c [Fe₂²⁺³⁺(H₂Hbamb)₂(*N*-MeIm)₂]I⁻. ^d [Fe₂³⁺(H₂Hbamb)(*N*-MeIm)₂](I⁻)₂. ^e For reactions with cyclohexane and cyclohexene, [Fe(TTP)Cl], ((5,10,15,20-tetra-*o*-tolylporphyrinato)iron(III) chloride).^{21,34} For reaction with methyl phenyl sulfide, (Fe(binaphthylporphyrin)Cl).^{21,34} For reaction with toluene, [Fe(TPP)Cl] ((tetraphenylporphyrinato)iron(III) chloride).²¹ ^f Turnover numbers corrected for non-metal-catalyzed products. Total product turnover are reported for porphyrin systems. ^g 100% efficiency represents one substrate oxygenation per iododibenzene consumed. ^h Yields are limited by amount of iododibenzene used in the reaction. ⁱ Catalyst:OIPh:substrate = 1:500:2500 ([catalyst] = 1 mM). All reactions were performed in 10% DMF/CH₂Cl₂ and followed for 12 h unless otherwise stated. ^j Catalyst:OIPh:substrate 1:10:210 ([catalyst] = 0.044 mM). All porphyrin reactions were performed in CH₂Cl₂. ^k Catalyst:OIPh:substrate = 1:5000:25000 ([catalyst] = 0.1 mM). ^l Catalyst:OIPh:substrate = 1:100:1000 ([catalyst] = 1 × 10⁻³ mM).²¹ ^m Catalyst:OIPh:substrate = 1:10:100 ([catalyst] = 1 × 10⁻³ mM).²¹

with their binuclear formulations.²⁵ Both **2** and **3** give rise to broadened *g* = 4.3 signals in their EPR spectra.

Catalytic atom transfer reactions (Table 1) were investigated under strict anaerobic conditions using OIPh as oxygen atom donor molecule and cyclohexane, cyclohexene, methyl phenyl sulfide, and toluene as substrates in 10% DMF/CH₂Cl₂.²⁸ All complexes were stable in the absence of iododibenzene for over 12 h. Parallel control reactions (absence of catalyst) were used to correct for non-metal-mediated products. Iodobenzene was recovered in quantitative yields in all reactions. The products obtained from the oxidation of cyclohexane with **1** and OIPh (cyclohexanol (57), cyclohexanone (1), and chlorocyclohexane (57)) clearly indicate the ability of **1** to catalyze the oxidation of alkanes. The effect of core oxidation states is evident from the reaction of **2**, which produces chlorocyclohexane (38) as the dominant product and only trace amounts of cyclohexanol (1). The fully oxidized complex, **3**, produces only low levels of chlorocyclohexane (13). The requirement for at least one ferrous center is more clearly evident in the catalytic oxidations of olefins such as cyclohexene. Both **1** and **2** yield primarily allylic oxidation products (cyclohexenol and cyclohexenone), although cyclohexene oxide represents a significant product (30% and 22%, respectively). Interestingly, reactions catalyzed by **3** produce only low levels of cyclohexenol, suggesting that the [Fe³⁺,Fe³⁺] core is not an effective oxygen transfer catalyst under these conditions. This conclusion is supported by results from the 2e⁻ catalytic oxidation of PhSMe where both **1** and **2** exhibit excellent catalytic ability while the diferric complex, **3**, is inert as a sulfide oxidation catalyst. The binuclear compound **1** oxidizes toluene to primarily produce benzylic oxidation products with only minor levels of product resulting from attack of the aromatic ring, while **2**, very interestingly, gives rise to predominantly aromatic ring oxidation products. Under identical conditions, simple Fe²⁺ and Fe³⁺ salts in the presence of OIPh were unable to catalyze any of these reactions.²⁹ The intermolecular kinetic isotope effect for alkane C–H oxidation was determined by the competitive oxidation of cyclohexane and cyclohexane-*d*₁₂ (*k*_H/*k*_D = 2.2).³⁰ This small intermolecular KIE is consistent with some,^{31–33} but not all,³⁴ studies for the oxidation of alkanes by MMO and is indicative of only a minor contribution from C–H bond breaking in the rate-determining step of substrate oxidation.

A comparison with the product distributions obtained from OIPh oxidation reactions catalyzed by iron porphyrins, whose

mechanisms invoke a reactive high-valent [Fe⁴⁺=O] species,^{21–23} is presented in Table 1. While Fe(TPP)Cl-catalyzed oxidations of cyclohexane do not form any chlorinated product in the presence of CH₂Cl₂, brominated products are reported in the reaction of cycloheptane in CH₂Br₂.³⁵ Furthermore, the ability of **1** and **2** to catalyze the oxidations of alkanes is substantially quenched when polar solvents such as CH₃CN are used instead of hydrophobic solvents such as CH₂Cl₂. An analogous phenomenon, ascribed to competition between solvent and the oxygen atom donor molecules for the labile site on the iron center, is also known for the porphyrin systems.³⁶ In the absence of substrate, **1** reacts with OIPh to yield a *μ*-oxo Fe³⁺ dimer, which is inert as an oxygen-atom transfer catalyst. Differences in the catalytic chemistry observed for **1** and **2** and that reported for [Fe₂²⁺(H₂Hbab)₂(*N*-MeIm)₂] are thought to reflect the greater ease by which the core redox properties induced by the H₂bamb²⁻ ligand support formation of the reactive intermediate.^{18,19}

These data demonstrate for the first time the ability of simple binuclear non-heme iron complexes containing at least one ferrous center to act as efficient oxygen-atom transfer catalysts using OIPh as the donor molecule. The chemistry exhibited by **1** and **2** clearly mimics many of the reactions heretofore seen only for heme systems, indicating that simple N/O ligand environments are adequate to support oxidative chemistry by oxygen atom donor molecules. Although the reactive intermediate(s) responsible for the observed alkane, arene, alkene, and sulfide oxidation chemistry exhibited by **1** and **2** is not as yet defined, its reactivity pattern is analogous to that observed for Cyt P-450, synthetic high-valent iron–oxo radical cation porphyrin model species,^{22,23} and the putative binuclear high-valent iron species observed in the catalytic cycle of MMO.^{4,5} Current efforts are designed to examine the effect of alternative oxygen-atom donors and metal-based redox potential on catalysis, elucidate the intimate mechanism of oxygen-atom transfer via isotopic labeling studies, and identify and spectroscopically characterize the reactive intermediate(s) responsible for this chemistry.

Supporting Information Available: Electrochemical UV/vis, and EPR spectroscopic characterization of **1**–**3** (5 pages). See any current masthead page for ordering and Internet access instructions.